Development of a photovoltaic array model for use in power-electronics simulation studies

J.A. Gow
C.D. Manning

Abstract: To be able to develop a complete solar photovoltaic power electronic conversion system in simulation, it is necessary to define a circuit-based simulation model for a PV cell in order to allow the interaction between a proposed converter (with its associated control arrangement) and the PV array to be studied. To do this it is necessary to approach the modelling process from the perspective of power electronics; that is to define the desired overall model in terms of the manner in which the electrical behaviour of the cell changes with respect to the environmental parameters of temperature and irradiance. The authors cover the development of a general model which can be implemented on simulation platforms such as PSPICE or SABER and is designed to be of use to power electronics specialists. The model accepts irradiance and temperature as variable parameters and outputs the I/V characteristic for that particular cell for the above conditions.

List of symbols

V = solar cell terminal voltage
I = solar cell terminal current
I_{ph} = photogenerated current (linear with irradiance)
I_{s1} = saturation current due to diffusion mechanism
I_{s1} = saturation current due to recombination in space-charge layer
A = 'diode quality' factor (variable with cell type for amorphous cells using the single exponential model, but for polycrystalline cells may be set constant to 2 across all cell types; approximation for Shockley–Read–Hall recombination in the space-charge layer [1])
R_s = cell series resistance
R_p = cell shunt resistance
e = electronic charge, 1.6×10^{-19} C
k = Boltzmann's constant, 1.38×10^{-23} J/K
V_g = band gap voltage, V
T = ambient temperature, Kelvin

IEE Proceedings online no. 19990116
DOI: 10.1049/ip-epa:19990116
Paper first received 6th May and in revised form 10th September 1998

The authors are with the Department of Electronic and Electrical Engineering, Loughborough University, Loughborough, Leicestershire, LE11 3TU, UK

1 Introduction

Photovoltaic systems research seems largely to be divided into two, fairly distinct areas; namely array physics, design and optimisation, and solar power conversion systems. This paper is not concerned with the design of the arrays but rather with development of a model of an array that is useful for power electronics applications. Better, more efficient converter systems may be developed by matching the control and drive requirements of the converter system to the characteristics of the array. Alternative energy specialists often appear not to have sufficient expertise in power electronics to be able to develop advanced converter systems, which can match the input characteristic of the power electronic system to those of the array, in order to make best use of the array. Examples of such non-optimal systems can be found in the field of solar array/battery combinations for stand-alone use [2–4] and in the area of utility interactive systems [5–8, 3].

A number of powerful component-based electronics simulation systems, such as SPICE and SABER, have become available over recent years, and such systems are often used during the development of power-electronics systems. In their basic form they do not provide a circuit model, or a component model, of the solar array itself, and thus are difficult to integrate with current electronics simulation technology used in the generic modelling of PV power electronic systems at a circuit level.

This paper presents a circuit-based simulation model of a PV array that can be implemented in any circuit-based simulation system such as SABER or SPICE. Such a model was not available prior to its development by the authors, and one was developed to fill this gap. This model of a PV array can be used in simulation studies of power electronic PV conversion systems.

2 Mathematical model for a photovoltaic cell

A mathematical description of the current/voltage (I/V) terminal characteristic for PV cells has been available for some time. The double-exponential eqn. 1, which models a PV cell, is derived from the physics of the p–n junction and is generally accepted as reflecting the behaviour of such cells, especially those constructed from polycrystalline silicon [9]. It is also suggested that cells constructed from amorphous silicon, usually using thick-film deposition techniques, do not exhibit as sharp a 'knee' in the curve as do the crystalline types, and therefore the current/voltage model of eqn. 2 provides a better fit to such cells. Eqn. 2 is in effect a subset of the double exponential equation effected by setting the second saturation current I_{s1} to zero. Both of these equations are implicit and nonlinear and there-

fore determination of an analytical solution is difficult.

$$I = I_{ph} - I_{s1}\left[e^{\frac{e(V+IR_s)}{kT}} - 1\right] - I_{s2}\left[e^{\frac{e(V+IR_s)}{AkT}} - 1\right] - \frac{V+IR_s}{R_{sh}} \quad (1)$$

$$I = I_{ph} - I_s\left(e^{\frac{e(V+IR_s)}{AkT}} - 1\right) - \frac{V+IR_s}{R_p} \quad (2)$$

Working backwards from the equations, an equivalent circuit can be easily determined, and this aids development of the simulation model. This equivalent circuit is shown in Fig. 1.

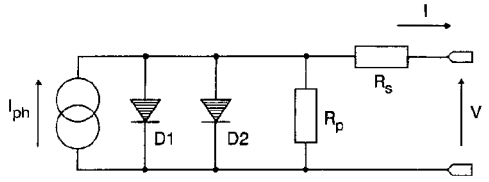

Fig. 1 *Cell equivalent circuit (double exponential model)*

Owing to the nature of these equations, there lies a problem in determining values for the five double-exponential model parameters which would be representative of those of a physical array system. Although it is not beyond the bounds of possibility to use the device physics to develop expressions for the *I/V* curve parameters, these would then only be in terms of semiconductor material constants and manufacturing variables such as doping densities. Most semiconductor constants vary quite considerably with production spread, are not provided on a manufacturer's data sheet and are also sometimes quite difficult to determine with accuracy.

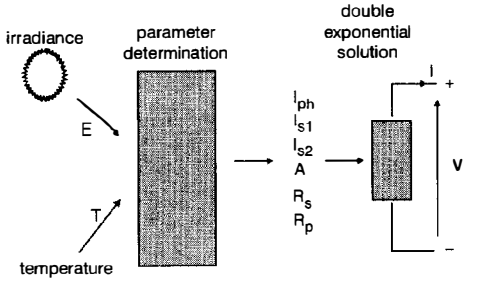

Fig. 2 *Basic modelling process*

The model behaves as a 'black box', in that the power electronics designer may select the desired values of the environmental parameters of irradiance and temperature, in order to study the operation of a converter system at either a fixed or a varying point upon the cell characteristics. To this end, eqn. 1 is of little use alone. It is necessary to relate the five variable parameters of the equation to the two environmental parameters. The essential modelling requirement is depicted in Fig. 2 and it can be seen to be a two-stage process. Firstly, the five parameters of the double-exponential equation must be determined from the cell type and the environmental parameters of irradiance and temperature and secondly, the double-exponential current–voltage equation may be solved in order to yield the electrical characteristics of the cell.

Solution of the double-exponential model equation for current in terms of voltage (or indeed vice-versa) is relatively straightforward, using iterative techniques, once the five parameters are known. These parameters will be different for each cell type, and will vary with the environmental parameters. It is necessary to define the law with which this variation takes place (for a given cell type) in order to complete the model. To do this a set of equations must be defined; the solution of which will relate each double-exponential model parameter, in turn, to the current values of irradiance and temperature, possibly incorporating constants which vary according to the specimen of array used.

2.1 Variation of double-exponential model parameters

Little appears to be known about the variation of the double-exponential equation parameters with respect to irradiance, with the exception of the photocurrent, which is known to be linear. However, the temperature variation is relatively simple to define. The general relations of the double exponential model parameters, with respect to temperature at a constant level of irradiance, can be obtained from p–n junction physics [10] and are shown in eqns. 3–7:

$$I_{ph} = I_{ph(nom)}(1 + K_0(T - 300)) \quad (3)$$

$$I_{s1} = K_1 T^3 e^{\left(-\frac{eV_g}{kT}\right)} \quad (4)$$

$$I_{s2} = K_2 T^{\frac{3}{2}} e^{\left(-\frac{eV_g}{2kT}\right)} \quad (5)$$

$$R_s = R_{s(nom)}[1 - K_3(T - 300)] \quad (6)$$

$$R_p = R_{p(nom)} e^{(-K_4 T)} \quad (7)$$

The constants K_0–K_4 are specific to a given specimen of cell, while the base parameters $I_{ph(nom)}$, $R_{s(nom)}$ and $R_{p(nom)}$ are values for the parameters at a temperature of 300 K. To complete the model it is necessary to modify eqns. 3–7 to take into account the variation of the five parameters with respect to irradiance. Irradiance and temperature could then be related mathematically to cell current and voltage, with no further variables of unknown behaviour being present. In order to define the modifications, it is necessary to analyse a quantity of PV cell current/voltage data over a range of irradiance and temperature, in order to determine the nature of the variation with irradiance. A data acquisition system was developed to facilitate the extraction of sets of *I/V* curve data from a sample solar cell at known values of temperature and irradiance. The system was designed to use a standard IBM compatible PC as the computational core. Software was developed to control the *I/V* data extraction process, and the additional hardware required to facilitate the measurement included the usual signal conditioning circuits and 12-bit ADCs.

2.2 Double exponential curve fitting

With the aforementioned *I/V* data acquisition system, it is possible to generate sets of *I/V* curves from a specimen solar cell across its operating range. However, in order to be able to determine the law linking irradiance and temperature to the five double-exponential model parameters, it is necessary to determine for each of the available *I/V* data sets a corresponding set of double exponential model parameters.

The double-exponential model equation is both non-linear, and implicit. To arrive at an analytical solution

of its five parameters, given a set of data at a specific temperature, is no easy task, and a better approach would be to look towards a numerical solution using curve fitting.

It was therefore decided to develop a PV-based curve-fitting system which is capable of running on a standard IBM compatible PC. The chosen method of solution of the PV curve was the Levenberg/Marquardt method [11], this being a robust method which exhibits sufficiently rapid convergence. The basic requirements of the method are shown in the flowchart of Fig. 3.

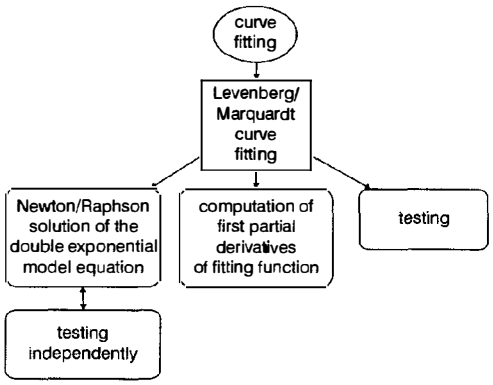

Fig. 3 *Basic requirements of the Levenberg–Marquardt curve fitting method*

The method requires a solution to the double-exponential model equation itself. As this equation is both nonlinear and implicit, a Newton–Raphson [11] iterative solution of the equation was used, arranged for current in terms of voltage.

The Levenberg–Marquardt method additionally requires solutions of the first partial derivatives of the function to be fitted with respect to each of the function parameters to be varied during the iterations. In the case of the double-exponential model such equations are simple to determine.

Since the Levenberg–Marquardt method is an iterative one, initial values will be required for each of the five variable parameters of eqn. 1, namely R_s, R_p, I_{s1}, I_{s2} and I_{ph} before the iteration can start. A is held constant, equal to 2, across the fit run for double exponential modelling.

The determination of the initial values is a nontrivial task, since inappropriate selection of initial values will result in nonconvergence of the algorithm. Considerable attention therefore needs to be paid to the correct selection of these initial values. In the following descriptions, initial values of the parameters are denoted by the subscript 0.

At $I = I_{sc}$, $V = 0$, I_{ph} is approximated well by I_{sc} as the portion of current flowing down the diodes and the parallel resistance is very small: R_s is small, therefore the voltage drop across it is also small. At $V = V_{oc}$, $I = 0$, the terms in R_s drop out of the equation, and the current flow in the parallel branches is dominated by the two diode currents. Therefore

$$I_{ph0} = I_{sc} \tag{8}$$

The saturation currents may then be approximated by making an assumption that these two currents are roughly equal as the cell voltage tends to zero, yielding eqns. 9 and 10.

$$I_{s10} = \frac{1}{2}\frac{I_{ph0}}{\left(e^{\left(\frac{eV_{oc}}{kT}\right)} - 1\right)} \tag{9}$$

$$I_{s20} = \frac{1}{2}\frac{I_{ph0}}{\left(e^{\left(\frac{eV_{oc}}{2kT}\right)} - 1\right)} \tag{10}$$

This leaves only R_{s0} and R_{p0} to be determined. Most of the approximations that could be used are derived in some way from eqn. 1, and thus rely upon the already approximated values of the other parameters. [1] presents a method based upon the use of the numerical values for the integral under the I/V and power curves, which appears to be valid; however, although the equations are dimensionally correct, it was found to be impossible to obtain sensible values for the resistances using them, often R_{p0} would end up negative. Eventually, a method involving the slope of the I/V curve at $V = V_{oc}$, at $V = 0$ and the value of I and V at the maximum power point was developed.

Experimentation with the I/V curve showed that R_s has a very marked effect upon the slope of the I/V curve at $V = V_{oc}$. R_p, however, has an effect upon the lateral position of the maximum power point together with a less marked effect upon the slope of the curve at $V = 0$, $I = I_{sc}$. To this end, the following system was developed. Eqn. 1 is differentiated and evaluated at $V = V_{oc}$, $I = 0$ and rearranged in terms of R_s to yield eqn. 11:

$$R_{s0} = -\left[\left.\frac{dV}{dI}\right|_{V_{oc}} + \frac{1}{\left(X_{1_v} + X_{2_v} + \frac{1}{R_p}\right)}\right] \tag{11}$$

where

$$X_{1_v} = \frac{eI_{s1}}{kT}e^{\left(\frac{eV_{oc}}{kT}\right)} \quad \text{and} \quad X_{2_v} = \frac{eI_{s2}}{AkT}e^{\left(\frac{eV_{oc}}{AkT}\right)}$$

Examination of eqn. 11 shows that in the neighbourhood of V_{oc} the terms X_{1v} and X_{2v} dominate over the much smaller $1/R_p$ and therefore the $1/R_p$ term may be neglected. The final equation for R_{s0} is given by eqn. 12

$$R_{s0} = -\left[\left.\frac{dV}{dI}\right|_{V_{oc}} + \frac{1}{X_{1_v} + X_{2_v}}\right] \tag{12}$$

In practice this gave good approximations for R_s.

A similar approach to that used in determining R_{s0} can be adapted to estimate R_p based upon the slope of the I/V curve at $I = I_{sc}$. However, the slope at this point does not bear as marked a dependence upon R_p as does the position of the maximum power point. Two methods were set up, and compared. The first of these involved evaluating eqn. 11 at $I = I_{sc}$, and rearranging in terms of R_p to give eqn. 13.

$$R_{p0} = -\left[\frac{1}{\frac{1}{\left(\left.\frac{dV}{dI}\right|_{I_{sc}} + R_s\right)} + X_{1_i} + X_{2_i}}\right] \tag{13}$$

where

$$X_{1_i} = \frac{I_{s1}}{nt}e^{\left(\frac{I_{sc}R_s}{nt}\right)} \quad \text{and} \quad X_{2_i} = \frac{I_{s2}}{Ant}e^{\left(\frac{I_{sc}R_s}{Ant}\right)}$$

The second of the two methods involved evaluating eqn. 1 at the maximum power point, using the approximated value of R_{s0}, and rearranging for R_{p0} to give eqn. 14.

$$R_{p0} = \frac{V_{mpp} + I_{mpp}R_{s0}}{I_{mpp} - I_{ph0} + I_{s10}\left(e^{\left(\frac{e(V_{mpp}+I_{mpp}R_{s0})}{kT}\right)} - 1\right) + I_{s20}\left(e^{\left(\frac{e(V_{mpp}+I_{mpp}R_{s0})}{AkT}\right)} - 1\right)} \quad (14)$$

Both systems gave a value of R_{p0} that resulted in convergence in most cases, but the approximation was not as good as that of R_{s0} from eqn. 12. This is not surprising as R_p is a parameter with a large value in comparison to the values of the other parameters, particularly the saturation currents. Small perturbations in the saturation currents can have a large influence upon the approximated value of R_{p0}. However, the reliability of convergence was better from the values calculated from eqn. 14 and this was used in the final implementation.

As with R_s, the convergence of R_{p0} was found to be slower for the cases of extremely low irradiance. This again is not surprising as R_p has greater dependence upon changes in other parameters; it is the largest and could be of the order of 10^{-3}, whereas the saturation currents are of the order of 10^{-12}. However, bad approximation leading to nonphysical convergence of the curve fitter was largely confined to regions of low irradiance. At present, initial values may be entered by hand should the computed method fail.

The system implements a heuristic algorithm based upon eqns. 13 and 14, with algorithm selection depending upon the curve data and success or failure of one or the other algorithms. If one algorithm fails, the other is attempted. If both methods fail on a difficult curve then values can still be entered by hand.

The final parameter to be determined is an initial value for A. In the double exponential model A is set to 2 and not allowed to vary during the curve fit, as this provides a first approximation for the Shockley-Read-Hall recombination current in the junction depletion region, and is acceptable for all practical cases (although the developed system does, in fact support single exponential modelling with A varying, this was not used during the tests).

In situations where the above methods for determining the initial values for R_s and R_p do not result in physically acceptable values, an alternative approach to the determination of initial values can be adapted. This is an iterative method, including within the iterative loop a better approximation for the two saturation currents and the photocurrent. It was seen that eqns. 12–14 could be placed in such a loop, with two additional equations determining the I_{ph} and $I_{s1/2}$ values. The equation sequence is given below in eqns. 15 and 16. Eqn. 15 gives the initial conditions, while eqn. 16 gives the equations solved in the iterative loop.

Initial condition equations:

$$R_{s0} = \left.\frac{dV}{dI}\right|_{V_{oc}}, \qquad R_{p0} = \left.\frac{dV}{dI}\right|_{I_{sc}}$$

$$I_{ph0} = I_{sc}, \qquad A_0 = 2$$

$$I_{s10} = \frac{I_{sc}}{2e^{\left(\frac{eV_{oc}}{kT}\right)} - 1}, \qquad I_{s20} = \frac{I_{sc}}{2e^{\left(\frac{eI_{sc}R_{s0}}{2kT}\right)} - 1} \quad (15)$$

Iterative loop equations:

$$X_{1_v} = \frac{I_{s1}}{vt}e^{\left(\frac{eV_{oc}}{kT}\right)}, \qquad X_{2_v} = \frac{I_{s2}}{Avt}e^{\left(\frac{eV_{oc}}{AkT}\right)}$$

$$R_{s0} = -\left[\left.\frac{dV}{dI}\right|_{V_{oc}} + \frac{1}{X_{1_v} + X_{2_v} + \frac{1}{R_p}}\right]$$

$$X_{1_i} = \left[\frac{I_{s1}}{vt}e^{\left(\frac{eI_{sc}R_{s0}}{kT}\right)}\right], \qquad X_{2_i} = \left[\frac{I_{s2}}{Avt}e^{\left(\frac{eI_{sc}R_{s0}}{AkT}\right)}\right]$$

$$R_{p0} = -\left[\frac{1}{\frac{1}{\left.\frac{dV}{dI}\right|_{I_{sc}} + R_{s0}} + X_{1_i} + X_{2_i}}\right] \quad (16)$$

An alternative iterative method makes use of the second of the two methods for the determination of R_p, i.e. eqn. 14, and involves placing this within an iterative loop. Together with equations to achieve a better solution of the saturation currents and the photocurrent, the iterative loop equations become

$$R_{p0} = \left[\frac{V_{mpp} + I_{mpp}R_{s0}}{I_{mpp} - I_{ph} + I_{s1}\left(e^{\left(\frac{e(V_{mpp}+I_{mpp}R_{s0})}{kT}\right)} - 1\right) + I_{s2}\left(e^{\left(\frac{e(V_{mpp}+I_{mpp}R_{s0})}{AkT}\right)} - 1\right)}\right]$$

$$I_{s20} = \left[\frac{I_{ph} - \frac{V_{oc}}{R_{p0}}}{e^{\left(\frac{eV_{oc}}{AkT}\right)} - 1}\right], \qquad I_{s10} = \left[\frac{I_{ph} - \frac{V_{oc}}{R_{p0}}}{e^{\left(\frac{eV_{oc}}{kT}\right)} - 1}\right]$$

$$I_{ph0} = I_{sc} + \frac{I_{sc}R_{s0}}{R_{p0}} + I_{s1}\left(e^{\left(\frac{eI_{sc}R_{s0}}{kT}\right)} - 1\right) + I_{s2}\left(e^{\left(\frac{eI_{sc}R_{s0}}{AkT}\right)} - 1\right) \quad (17)$$

Essentially, the iterative methods place the existing static solutions of R_{p0} and R_{s0} within an iterative loop. Each iteration arrives at a better approximation of the parameters. Once again the software uses a heuristic implementation of the initial parameter value extraction. if the static methods (eqns. 12 and 13) fail to deliver sensible initial condition values (> 0) the alternative iterative methods (eqn. 15 with eqn. 16, eqn. 15 with eqn. 17) are also tried in turn. If these fail the software prompts for manual input of initial values. Once sensible values for initial parameter values are determined by one means or another, the curve-fitter is then called. The data set is rejected if the curve-fitter again fails to converge or returns unacceptable parameter values.

2.3 Double exponential model parameter determination

Referring to Fig. 2, it can be seen that the modelling process requires firstly the determination of the double-exponential equation parameters for the cell at each specific value of irradiance and temperature. This was achieved by implementing a first-level fit of the double exponential parameters to the I/V data sets using the method described in Section 2.2. An example of this can be seen in Fig. 4. This shows an experimental I/V

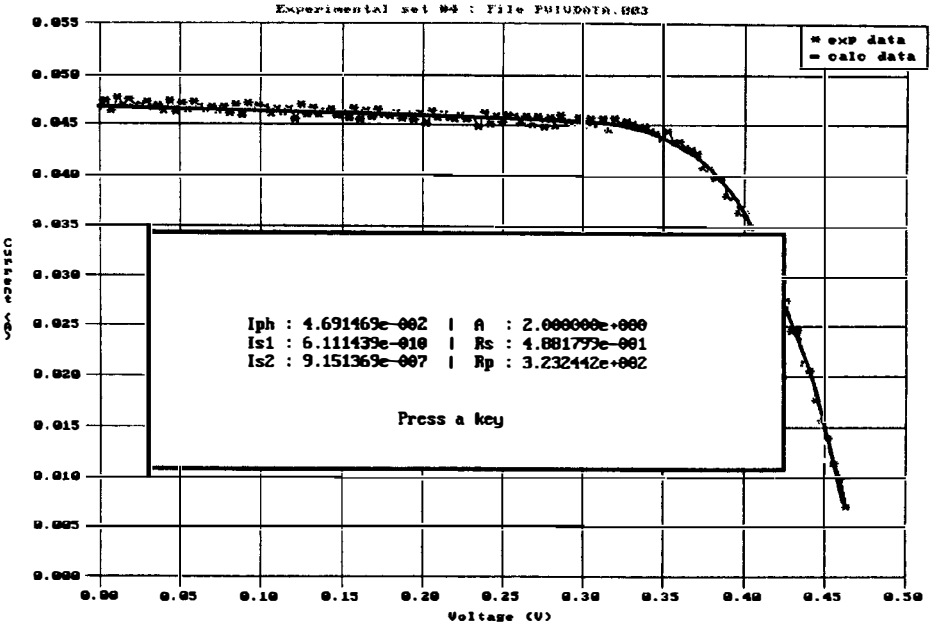

Fig. 4 *Fitted data superimposed upon 'raw' data*

Table 1: Table of constants for the polycrystalline cell used in the tests

Parameter	Constant values		
I_{ph}	$K_0 = -5.729 \times 10^{-7}$	$K_1 = -0.1098$	
I_{s1}	$K_2 = 44.5355$	$K_3 = -1.264 \times 10^4$	
I_{s2}	$K_4 = 11.8003$	$K_5 = -7.3174 \times 10^3$	
A	$K_6 = 2$	$K_7 = 0$	
R_s	$K_8 = 1.47$	$K_9 = 1.6126 \times 10^3$	$K_{10} = -4.474 \times 10^{-3}$
R_p	$K_{11} = 2.303 \times 10^6$	$K_{12} = -2.812 \times 10^{-2}$	

curve. Superimposed upon the experimental curve is an I/V curve back-calculated from the double-exponential model parameters given, together with the values of the parameters themselves.

2.4 Generation of equations relating the double exponential model parameters to irradiance and temperature

Equations relating the double-exponential equation parameters to temperature have been published [10]. These equations give the variation of the parameters with respect to temperature only. They do not take into account effects of changes in irradiance. They are therefore unsuitable in their present form for use in a general-purpose PV modelling system where both temperature and irradiance may vary. A new set of equations was developed incorporating irradiance terms for those parameters that are affected by irradiance. The equations were developed as described below.

Firstly, the double exponential equation parameters, extracted as described in Section 2.2, were plotted against temperature and irradiance; the plot being used as an aid to determine the nature of the relationships involved. Taking the parameters in turn one by one and determining the optimum relationship, the following equations were derived using a combination of proposed equations and curve fitting, in which the optimum fit is the one in which the chi-squared [11] value was at a minimum. Accordingly, the equations so produced are given below in eqns. 18–23. Since A is held at 2, the constants K_6 and K_7 are set at 2 and 0, respectively.

$$I_{ph} = K_0 E(1 + K_1 T) \tag{18}$$

$$I_{s1} = K_2 T^3 e^{\left(\frac{K_3}{T}\right)} \tag{19}$$

$$I_{s2} = K_4 T^{\frac{3}{2}} e^{\left(\frac{K_5}{T}\right)} \tag{20}$$

$$A = K_6 + K_7 T \tag{21}$$

$$R_s = K_8 + \frac{K_9}{E} + K_{10} T \tag{22}$$

$$R_p = K_{11} e^{(K_{12} T)} \tag{23}$$

The equations are applicable to any PV cell which satisfies the double-exponential model. It can be seen that the equations contain a total of thirteen constants, these constants being specific to the cell that has been characterised by the system. Table 1 lists the values of the constants for a sample of a polycrystalline cell used during the experiment.

Figs. 5–9 show the experimentally extracted values of the double exponential model parameters superimposed upon values generated from the model equations.

2.5 Circuit-level model

The modelling system developed is based around the characteristics of a single PV cell. The models of the cells are such that if connected in an array the array

can be treated (mathematically) as a single cell with multipliers incorporated accordingly, dependent upon the number of series/parallel chains in the array. This only holds if the irradiance and temperature are constant across the entire surface of the array. For a small array (c. $1\,m^2$) this is likely to be true. However, for a field of arrays such as encountered in a large photovoltaic plant, this may well not be the case, and the simulated array would have to be constructed from discrete cell templates each representing the appropriate combination of cells, as necessary. Fig. 10 shows the arrangement of an $m \times n$ array, while Fig. 11 shows the decomposition for a 2 × 3 array as an example.

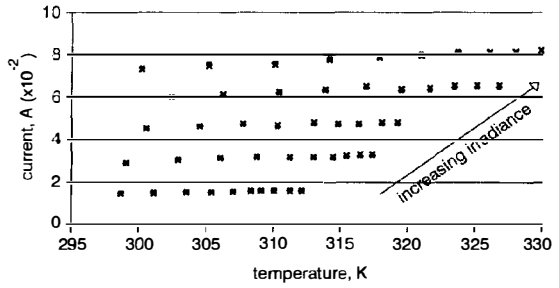

Fig. 5 *Variation of I_{ph} with temperature and irradiance, together with fitted points.*
● I_{ph}
× calculated I_{ph}

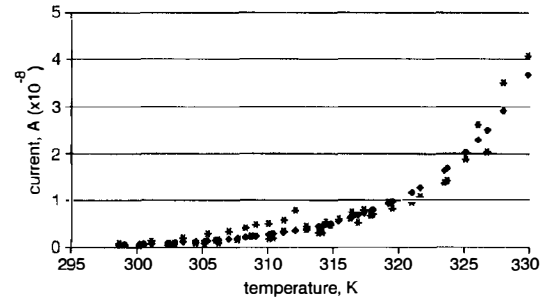

Fig. 6 *Variation of all values of I_{s1} with temperature, together with corresponding fitted points*
* I_{s1}
◆ calculated I_{s1}

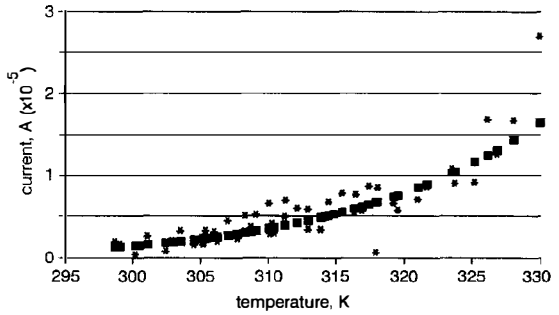

Fig. 7 *Variation of all values of I_{s2} with temperature, including corresponding fitted points*
* I_{s2}
■ calculated I_{s2}

The parameters add by superposition to an extent, with the exception of the two diode currents. As these are nonlinear, a multiplier N_s must be placed within the exponential term. Depending upon the design and dimensions of the array it may be possible to simulate the array by collapsing the series chains into a number of parallelled modelling units or, in the case of a large plant, the best approach may be to collapse the model of each panel into a single modelling unit, as the irradiance, and hence the temperature, is unlikely to change across the dimensions of a single panel but could possibly change across the plant in its entirety. Either way, the modelling system opted for gives the greatest flexibility in the manner in which the array may be simulated; the effect of a cloud passing could be simulated by reducing and increasing the irradiance across the plant in a 'Mexican wave' fashion, for example.

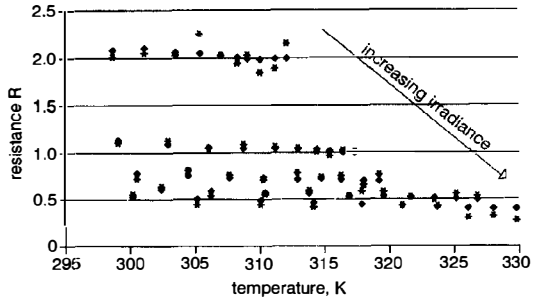

Fig. 8 *Variation of R_s with temperature, with corresponding fitted points superimposed*
* R_s
◆ calculated R_s

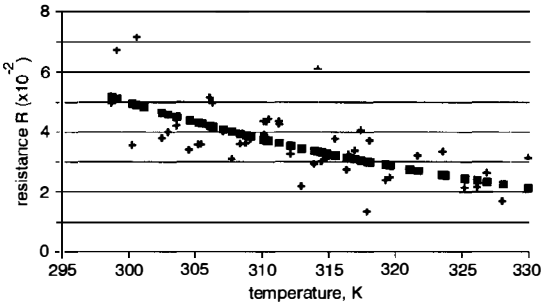

Fig. 9 *Variation of R_p with temperature, with corresponding fitted points superimposed*
+ R_p, experimental
■ R_p, calculated

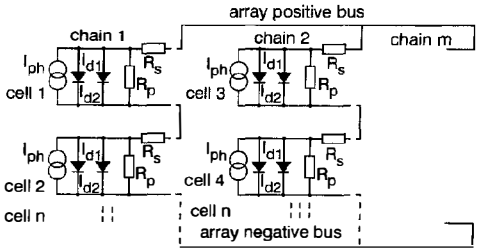

Fig. 10 *Cell connections forming an array*

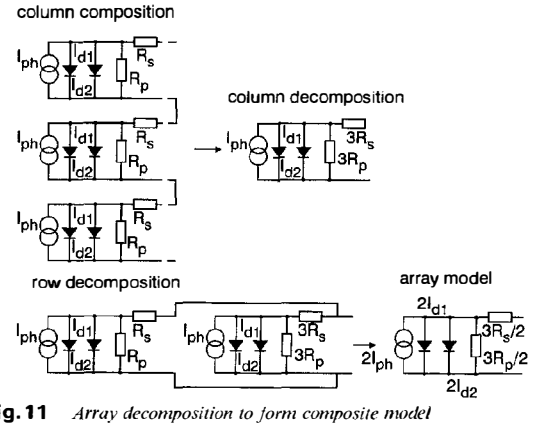

Fig. 11 *Array decomposition to form composite model*

In Figs. 10 and 11 the two diode currents I_{d1} and I_{d2} are the solution of the second and third exponential terms in eqn. 1; thus in the composite models, to represent series chains, the IV equation must incorporate the N_s multiplier. The complete multidimensional array model equation is shown in eqn. 24 below,

$$I = N_p \left[I_{ph} - I_{s1} \left(e^{\frac{e\left[\left(\frac{V}{N_s}\right)+\left(\frac{I}{N_p}\right)R_s\right]}{kT}} - 1 \right) - I_{s2} \left(e^{\frac{e\left[\left(\frac{V}{N_s}\right)+\left(\frac{I}{N_p}\right)R_s\right]}{AkT}} - 1 \right) - \frac{\left(\frac{V}{N_s}\right)+\left(\frac{I}{N_p}\right)R_s}{R_p} \right] \quad (24)$$

where N_s and N_p are the number of series cells, and the number of parallel cells, respectively.

The actual implementation in SPICE or SABER is very straightforward, consisting of a solution to eqns. 18–23 followed by a solution to eqn. 24. The constants K_0–K_{12}, together with the environmental variables temperature and irradiance, are passed to the cell template through fields in a solar-cell schematic symbol, designed for the appropriate schematic-capture utility front-end for the simulator. For example, the PV cell symbol using the SABER simulator is shown in Fig. 12. Note that for the case of SABER, temperature is a global parameter within the framework of the simulator and does not have to be specified to each template through the parameter list.

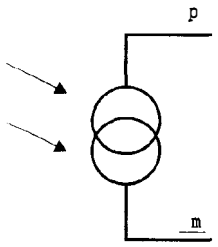


```
K0:*req*
K1:*req*
K2:*req*
K3:*req*
K4:*req*
K5:*req*
K6:*req*
K7:*req*
K8:*req*
K9:*req*
K10:*req*
K11:*req*

K12:*req*
EI:*req*
nseries:*req*
nparallel:*req*
```

Fig.12 *PV cell symbol using DesignStar in SABER*

2.7 SABER model result

The SABER model was used to demonstrate the performance of the modelling process. Fig. 13 shows a sample data set from those extracted from the cell including the power curve for the cell. The I/V and power data back calculated from the model is also superimposed upon the curve and serves to show the accuracy of the fit. Fig. 14 is an I/V sweep taken from the SABER model at the same irradiance and temperature as Fig. 13, and using the constant K_0–K_{12} set extracted. It can be seen that the curves are virtually identical.

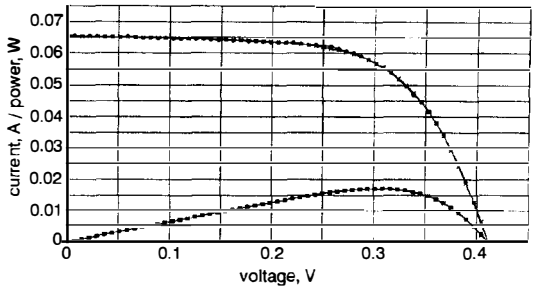

Fig.13 *Experimental I/V data at irradiance 3291, temperature 326.8K*
○ experimental data
× calculated data
* experimental power
□ calculated power

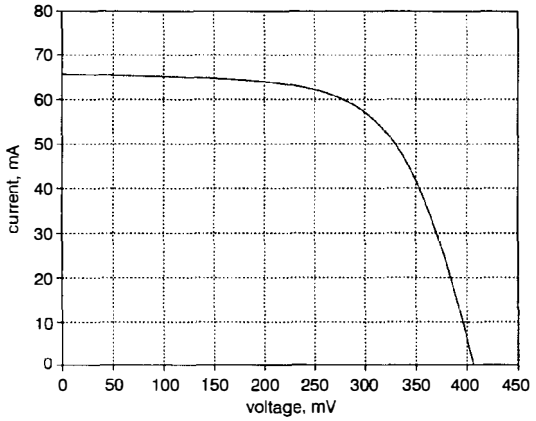

Fig.14 *I/V sweep obtained from SABER template using extracted parameters at irradiance 3291, temperature 326.8K*

3 Conclusions

A model suitable for use by power electronics specialists has been developed, and has been designed for easy implementation on simulation platforms such as SPICE or SABER. The model accepts irradiance and temperature as input parameters and outputs the I/V characteristic for the cell for the above conditions. This model can be applied to photovoltaic cell types whose device physics conform to double-exponential behaviour. Using the modelling system presented in the paper, cell samples may be characterised to obtain a set of constants. If these constants are submitted to a circuit-level simulation template the electrical behaviour of arrays of cells may be simulated across the range of irradiance and temperature for which the model has been defined. In the context of power electronics, there is now available a model for a photovoltaic array installation, which will allow the effects of varying irradiance and temperature to be simulated in conjunction with a power conversion system. This will enable the behaviour of the power conversion system to be analysed and optimised for operation in the field of solar photovoltaic power conversion.

4 References

1 GLYNN, L.W., McDERMOTT, J.K., and OSS, J.P.: 'SABER digital computer simulation of an electrical power subsystem'. Proceedings of the 23rd Intersociety Energy Conversion Engineering conference, 1988, pp. 543–546

2 TANAKA, K., SAKOGUCHI, E., FUKUDA, Y., TAKEOKA, A., and TOKIZAKI, H.: 'Residential solar powered air conditioner'. Proceedings of the 1993 European conference on *Power electronics*, Brighton, England, 1993, pp. 127–132

3 DUARTE, J.L., WIJNTJENS, J.A.A., and ROZENBOOM, J.: 'Designing light sources for solar powered systems'. Proceedings of the 1993 European conference on *Power electronics*, Brighton, England, 1993, pp. 78–82

4 SAVARY, P., NAKAOKA, M., and MARUHASHI, T.: 'Novel type of high frequency link inverter for photovoltaic residential applications', *IEE Proc. B, Electr. Power Appl.*, 1986, **133**, (4), pp. 279–284

5 CHIANESE, D., CAMANI, M., CEPPI, P., and IACOBUCCI, D.: 'TISO: 4kW experimental amorphous silicon PV power plant'. Proceedings of the 10th European conference on *Photovoltaic solar energy*, Lisbon, Portugal, 1991, pp. 755–758

6 NENTWICH, A., SCHNEEBERGER, M., SZELESS, A., and WILK, H.: '30kW photovoltaic plant in the Alps of Austria'. Proceedings of the 10th European *Photovoltaic solar energy* conference, Lisbon, Portugal, 1991, pp. 766–770

7 CORVI, C., VIGOTTI, R., ILICETO, A., and PREVI, A.: 'ENEL's 3MW PV power station preliminary design'. Proceedings of the 10th European *Photovoltaic solar energy* conference, Lisbon, Portugal, 1991, pp. 1277–1280

8 TANAKA, K., SAKOGUCHI, E., FUKUDA, Y., TAKEOKA, A., and TOKIZAKI, H.: 'Residential solar powered air conditioner'. Proceedings of the 1993 European conference on *Power electronics*, Brighton, England, 1993, pp. 127–132

9 PROTOGEROPOULOS, C., BRINKWORTH, B.J., MARSHALL, R.H., and CROSS, B.M.: 'Evaluation of two theoretical models in simulating the performance of amorphous silicon solar cells'. Proceedings of the 10th European *Photovoltaic solar energy* conference, Lisbon, Portugal, 1991, pp. 412–415

10 VEISSID, N., and DE ANDRADE, A.M.: 'The I-V silicon solar cell characteristic parameters temperature dependence, an experimental study using the standard deviation method'. Proceedings of the 10th European *Photovoltaic solar energy* conference, Lisbon, Portugal, 1991, pp. 43–47

11 PRESS, W.H., TEUKOLSKY, S.A.., VETTERLING, FLANNERY, B.P.: 'Numerical recipes in C - the art of scientific computing' (Cambridge University Press, 1992, 2nd edn.)